Ordering parameter and band-offset determination for ordered $Ga_xIn_{1-x}P/(Al_{0.66}Ga_{0.34})_yIn_{1-y}P$ quantum wells

Jun Shao*
4. Physikalisches Institut, Universität Stuttgart, D-70550 Stuttgart, Germany
and National Lab for Infrared Physics, Shanghai Institute of Technical Physics, Chinese Academy of Sciences, 200083 Shanghai, China

Achim Dörnen, Rolf Winterhoff, and Ferdinand Scholz
4. Physikalisches Institut, Universität Stuttgart, D-70550 Stuttgart, Germany
(Received 24 September 2001; revised manuscript received 08 April 2002; published 10 July 2002)

Low-temperature (1.8 K) optical reflectivity measurements have been carried out to identify the principal interband transition energies in ordered $Ga_xIn_{1-x}P/(Al_{0.66}Ga_{0.34})_yIn_{1-y}P$ quantum well (QW) samples. To account for ordering effects on the band offset and optical transition energy, a theoretical model has been constructed by incorporating the CuPt-type ordering effects of band-gap reduction $[\Delta E_g(\eta)]$ and valence-band splitting $[\Delta^O_{111}(\eta)]$ into the model-solid theory. Fitting of the observed transition energies to the calculations indicates that the model can reasonably describe the band-to-band transitions in the ordered QW's. Conclusions are reached that show that (i) ordering parameters in the QW's can be estimated with the first band-to-band transition energy. (ii) Among the $\Delta E_g(1)$ values available in the literature, two combinations $\Delta E_g(1)/\Delta^O_{111}(1)$ of -0.43 eV/0.16 eV and -0.471 eV/0.20 eV lead to good descriptions of the lattice-matched QW's. For the compressively strained samples, however, a smaller absolute value of $\Delta E_g(1)$ is favorable. Compressive strain tends to weaken the ordering effects. (iii) For a disordered and lattice-matched/compressively strained QW, the conduction-band-offset ratio has a nearly constant value of $Q_c \sim 0.58$. (iv) Ordering causes an increase in Q_c, and for lattice-matched and compressively strained QW's Q_c falls in a range of $0.58-0.72$ as η changes from 0 through 1. The influence is checked by using different values of the valence- and conduction-band deformation potentials in the calculations. A comparison of Q_c is also made with previously reported values.

DOI: 10.1103/PhysRevB.66.035109 PACS number(s): 71.15.−m, 71.35.Cc, 73.21.Fg, 78.30.Fs

I. INTRODUCTION

$Ga_xIn_{1-x}P$/AlGaInP heterostructures represent the largest direct band gap in the III-V low-dimensional semiconductor system apart from nitrogen containing compounds. They possess great potential for visible electron-optical applications, such as ultrabright red-green light-emitting diodes, and semiconductor lasers.[1–4] To aid the device design and modeling, knowledge of material properties, e.g., band offsets and band-edge carrier effective masses, is crucially important.

It has been well established that, under proper growth conditions, epitaxially grown $Ga_xIn_{1-x}P$ exhibits CuPt-type ordering along the $[111]_B$ directions. The ordering-induced changes in the band structure of the $Ga_xIn_{1-x}P$ bulk alloy have been investigated both experimentally and theoretically.[5–14] Recently, a general theory was presented explaining how the strain produced by lattice mismatch with the substrate interacts with ordering effects.[11,12] On the other hand, while the band-edge electronic structure in strained $Ga_xIn_{1-x}P$/AlGaInP quantum wens (QW's) has been intensively studied,[15–20] ordering effects which could be used to optimize optoelectronic devices[21] were not included.

In this work, we closely follow ordering theory[11,12] and model-solid theory[22–24] in describing total effects of ordering and strain on the valence- and conduction-band edges in ordered $Ga_xIn_{1-x}P$/AlGaInP QW's. We measure ordered and strained/lattice-matched $Ga_xIn_{1-x}P/(Al_{0.66}Ga_{0.34})_yIn_{1-y}P$ QW samples by optical reflectivity spectroscopy to determine excitonic resonance energies.

The results indicate that (i) the theoretical model can well describe band-to-band transitions in ordered QW's. (ii) Fitting the first band-to-band transition energy to the theoretical simulation can lead to a reasonable evaluation of the ordering parameter in QW's. (iii) While Wei and Zunger's values of $\Delta E_g(1) = -0.43$ eV and $\Delta^O_{111}(1) = 0.16$ eV can well explain the lattice-matched samples, a smaller absolute value of $\Delta E_g(1)$ is favorable for the compressively strained samples. Compressive strain tends to weaken the ordering effect. (iv) Ordering causes the conduction-band-offset ratio Q_c to increase, especially under lattice-matched and tensile strained conditions. (v) For disordered and lattice-matched/compressively strained QW's, Q_c has a relatively constant value, $Q_c \sim 0.58$.

II. THEORETICAL CALCULATION OF THE BAND-EDGE ELECTRONIC STRUCTURE

Atomic CuPt-type ordering results in two prominent effects to electronic band structures: band-gap reduction and valence-band splitting. The valence-band splitting is just like that caused by spin-orbit interaction, and can be described using a parameter similar to Δ^{SO} (spin-orbit splitting),[11,12]

$$\Delta^O_{111}(\eta) = \eta^2 \Delta^O_{111}(1), \tag{1}$$

where η is ordering parameter, $\Delta^O_{111}(\eta)$ is the crystal-field splitting due to the atomic ordering, and $\Delta^O_{111}(1)$ is the value of a perfectly ordered alloy. The band-gap reduction is mainly due to a depression of the Γ^c_6 conduction band caused by the folding state from the L point.[5,6,12] The ordering-induced valence-band splitting also plays a minor role as it shifts the upper valence-subband upward.[25] The band-gap reduction can be described as

$$dE_g(\eta)=\eta^2\Delta E_g(1), \tag{2}$$

where $\Delta E_g(1)$ is band-gap reduction of the perfectly ordered alloy relative to the perfectly random alloy. Neither $\Delta E_g(1)$ nor $\Delta^O_{111}(1)$ is uniquely available in the literature, e.g., Wei *et al.* previously reported[7,8] $\Delta E_g(1)=-0.32$ eV and $\Delta^O_{111}(1)=0.20$ eV based on first-principles, local-density approximation (LDA), and recently suggested $\Delta E_g(1)=-0.43$ eV and $\Delta^O_{111}(1)=0.16$ eV using a LDA-corrected method for strain-free alloy;[26] Ernst *et al.* extracted a value of $\Delta E_g(1)=-0.471$ eV from photoluminescence excitation (PLE) measurements;[13,14] Geng proposed a value of -0.405 eV for a compressively strained QW.[27] Their influence on the electronic band-structure calculation will be checked in Sec. IV.

Incorporating the two effects into model-solid theory,[22–24] a general description of the band lineup in the $Ga_xIn_{1-x}P$ QW layer including the interaction of (111) CuPt-type ordering with (001) strain as well as spin-orbit split-off (SO) states is obtained:

$$\begin{aligned} E_{v,i}&=E_{v,\mathrm{av}}+dE_{v,\mathrm{av}}+E_i \quad (i=1,2,3),\\ E_c&=E_{v,\mathrm{av}}+dE_c+E_g(\epsilon=0,\eta=0)+dE_g(\eta)\\ &\quad+\frac{1}{3}[\Delta^{\mathrm{SO}}+\Delta^O_{111}(\eta)], \end{aligned} \tag{3}$$

where $E_{v,\mathrm{av}}$ is the weighted average energy over the three uppermost valence bands at the Γ point and taken as a reference energy level.[22] $dE_{v,\mathrm{av}}$ and dE_c are energy shifts of $E_{v,\mathrm{av}}$ and E_c induced by the hydrostatic strain component and can be expressed as

$$dE_{v,\mathrm{av}}=2a_v\frac{C_{11}-C_{12}}{C_{11}}e_{xx}, \quad dE_c=2a_c\frac{C_{11}-C_{12}}{C_{11}}e_{xx};$$

a_v and a_c are the hydrostatic deformation potentials of the valence and conduction band, respectively. $e_{xx}=(a_s-a_f)/a_f$. a_s is the lattice parameter of the substrate, and a_f is the value of QW layer. E_i are valence-subband shifts relative to their weighted average caused by both the uniaxial strain component and atomic ordering, and correspond to the eigenvalue of the Hamiltonian:[12]

$$\mathbf{H_v}=\frac{1}{3}\begin{pmatrix} \Delta^S_{001} & -\Delta^O_{111}-i\Delta^{\mathrm{SO}} & -\Delta^O_{111} & 0 & 0 & \Delta^{\mathrm{SO}} \\ -\Delta^O_{111}+i\Delta^{\mathrm{SO}} & \Delta^S_{001} & -\Delta^O_{111} & 0 & 0 & -i\Delta^{\mathrm{SO}} \\ -\Delta^O_{111} & -\Delta^O_{111} & -2\Delta^S_{001} & -\Delta^{\mathrm{SO}} & i\Delta^{\mathrm{SO}} & 0 \\ 0 & 0 & -\Delta^{\mathrm{SO}} & \Delta^S_{001} & -\Delta^O_{111}+i\Delta^{\mathrm{SO}} & -\Delta^O_{111} \\ 0 & 0 & -i\Delta^{\mathrm{SO}} & -\Delta^O_{111}-i\Delta^{\mathrm{SO}} & \Delta^S_{001} & -\Delta^O_{111} \\ \Delta^{\mathrm{SO}} & i\Delta^{\mathrm{SO}} & 0 & -\Delta^O_{111} & -\Delta^O_{111} & -2\Delta^S_{001} \end{pmatrix} \tag{4}$$

with

$$\Delta^S_{001}=3b\frac{C_{11}+2C_{12}}{C_{11}}e_{xx}.$$

$E_g(\epsilon=0,\eta=0)$ is the band gap of the strain-free and totally random $Ga_xIn_{1-x}P$ alloy and is adopted from Ref. 28.

The band lineup for the $(Al_{0.66}Ga_{0.34})_yIn_{1-y}P$ barrier layer can be expressed as being similar to that of $Ga_xIn_{1-x}P$, but it ignores the ordering effect. That is, for the first two valence subbands, i.e., heavy-hole (hh) and light-hole (lh) subbands, the E_i in Eq. (3) can be described as[12,22,24]

$$E_1(\mathrm{barrier})=\frac{\Delta^{\mathrm{SO}}}{3}+\frac{\Delta^S_{001}}{3},$$

$$E_2(\mathrm{barrier})=-\frac{\Delta^{\mathrm{SO}}}{6}-\frac{\Delta^S_{001}}{6}+\frac{1}{2}\left[(\Delta^{\mathrm{SO}})^2-\frac{2}{3}\Delta^{\mathrm{SO}}\Delta^S_{001}+(\Delta^S_{001})^2\right]^{1/2}. \tag{5}$$

Here only the value E_i(barrier) of the upper valence subband is usedto obtain E_v(barrier). The band gap of the strain- and ordering-free $(Al_{0.66}Ga_{0.34})_yIn_{1-y}P$ alloy is also adopted from Ref. 28.

The material parameters used for the modeling are listed in Table I. Parameters for the ternary and quaternary are linearly interpolated between the binary values, expect for $E_{v,\mathrm{av}}$, for which a bowing parameter is taken into account.[28] For the hydrostatic deformation potentials, a set of values newly calculated by Wei and Zunger[29] with the LDA method is listed in the parentheses in addition to the values widely used in the literature. It's distinct that the new values of a_v

TABLE I. Material parameters used in the band-edge electronic structure calculations. The values of the a_v and a_c listed in the parentheses are recently reported by Wei and Zunger. (Ref. 29). c_{11} and c_{12} are in units of 10^{11} dyn/cm^2.

Name	a_v (eV)	a_c (eV)	b (eV)	C_{11}	C_{12}	a (Å)	$E_{v,\mathrm{av}}$ (eV)	Δ^{SO} (eV)
AlP	3.15 (2.64)	−5.54 (−5.86)	−1.6	13.2	6.30	5.462	−8.09	0.07
GaP	1.70 (−0.58)	−7.14 (−8.57)	−1.5	14.39	6.52	5.45	−7.40	0.08
InP	1.27 (−0.41)	−5.04 (−5.71)	−1.6	10.22	5.76	5.8686	−7.04	0.11

for GaP and InP have an opposite sign relative to the widely used ones. In this work, the major discussion will be based on the widely used values to simplify the comparison with the band-offset values available in the literature, though the difference caused by using the new values will also be addressed in Sec. IV.

The band-gap offsets and band-offset ratios of ordered $Ga_xIn_{1-x}P/(Al_{0.66}Ga_{0.34})_yIn_{1-y}P$ QW are

$$\Delta E_c = E_c(\text{barrier}) - E_c,$$

$$\Delta E_{v,i} = E_{v,i} - E_v(\text{barrier}),$$

$$Q_c = \frac{\Delta E_c}{\Delta E_c + \max(\Delta E_{v,i})}, \tag{6}$$

where $\max(\Delta E_{v,i})$ is the confinement of the upper valence subband, which is hh-like for lattice match and compressive strain, and is lh-like for tensile strain.

To determine confinement energies in the QW, a finite-deep square-well model is employed, which leads to

$$E^z_{s,n} = \Delta E_s \times \left(\frac{m^*_{s,\mathrm{w}}}{m^*_{s,\mathrm{w}} + m^*_{s,\mathrm{b}} \tan^2(k_{s,n}L/2)} \right)^{1/2}$$

for $\tan(k_{s,n}L/2) > 0$, and

$$E^z_{s,n} = \Delta E_s \times \left(\frac{m^*_{s,\mathrm{w}}}{m^*_{s,\mathrm{w}} + m^*_{s,\mathrm{b}} / \tan^2(k_{s,n}L/2)} \right)^{1/2}$$

for $\tan(k_{s,n}L/2) < 0$. s refers to the conduction (e) or valence (h_1, h_2, h_3) subband. w and b refer to the well and barrier material, respectively. L is the well width, and ΔE_s is the potential well height, which is given by Eq. (6); $m^*_{s,\mathrm{w}}$ and $m^*_{s,\mathrm{b}}$ are effective masses in the well and barrier, respectively, and are listed in Table II.

Finally all the three band-to-band (i.e., e-h_1, e-h_2, e-h_3) transition energies are obtained:

$$E_{i,n} = E^z_{e,n} + |E^z_{h_i,n}| + E_c - E_{v,i} \quad (i = 1,2,3) \tag{7}$$

and the energy difference between the first two transitions is also straightforward,

$$\Delta E_{12} = E_{1,1} - E_{2,1}. \tag{8}$$

III. EXPERIMENT

Three series of $Ga_xIn_{1-x}P/(Al_{0.66}Ga_{0.34})_yIn_{1-y}P$ QW's, each consisting of three samples grown on (001) GaAs substrates with different misorientation, i.e., 0°, 6° off toward $[111]_A$, and 6° off toward $[111]_B$, respectively, are investigated in this work. They were prepared by metal-organic vapor-phase epitaxy at a temperature of 700 °C. The first two series, A and B, have a similar structure: on top of the Si-doped GaAs substrate, a 30-nm-thick GaAs buffer layer was grown, followed by a 2-nm-thick GaInP layer and a 20-nm-thick $(Al_{0.66}Ga_{0.34})_{0.52}In_{0.48}P$ layer, then 10 periods of 10-nm-GaInP/4-nm-$(Al_{0.66}Ga_{0.34})_yIn_{1-y}P$ QW's were grown, with a 50-nm-thick $(Al_{0.66}Ga_{0.34})_{0.52}In_{0.48}P$ buffer layer and a 2-nm-thick GaInP cap layer at the end of the structure. The only difference is that the A series was lattice matched ($x \simeq 0.52$, $y = 0.52$), whereas the B series had a compressively strained QW layer and a tensile strained barrier layer ($x = 0.40$, $y = 0.76$). The third series, C, is similar to the A series but had a 410-nm-thick Zn-doped GaP capping layer.

Optical reflectivity spectra were recorded at a temperature of 1.8 K by using a BOMEMDA 3.01 Fourier-transformed-infrared spectrometer. The system was equipped with a conventional halogen lamp, a quartz beam splitter, and a silicon-diode detector. With this optical configuration, a spectro-

TABLE II. Out-of-plane effective masses used in the calculations. li. stands for linear interpolation.

Name	GaP	InP	AlP	$Ga_{0.5}In_{0.5}P$	(AlGa)InP
m^z_e/m_0	0.15 [a]	0.064 [a]	0.22 [a]	0.088 [b]	li.
m^z_{hh}/m_0	0.41 [a]	0.48 [a]	0.52 [a]	0.48 [c]	li.
m^z_{lh}/m_0	0.16 [a]	0.14 [a]	0.22 [a]	0.14 [c]	li.
m^z_{so}/m_0	0.23 [a]	0.19 [a]	0.34 [a]	0.226 [c]	li.

[a]Reference 23.
[b]Reference 30.
[c]Reference 16.

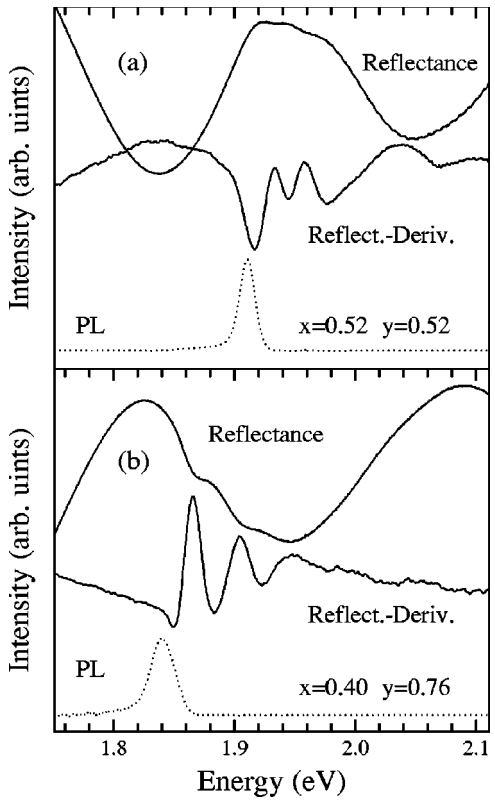

FIG. 1. Reflectivity spectra and their second-order derivatives for (a) lattice-matched and (b) compressively strained $Ga_xIn_{1-x}P/(Al_{0.66}Ga_{0.34})_yIn_{1-y}P$ QW's, respectively. PL spectra are plotted as dotted-lines to aid the identification of the QW-related transitions in the reflectivity spectra.

scopic range of $10\,000-18\,500\ cm^{-1}$ and a resolution of $6\ cm^{-1}$ ($\sim$0.7 meV) were accessible.

In Fig. 1 representative reflectivity spectra are depicted for lattice-matched and compressively strained samples, respectively. To enable a comparison the corresponding PL spectra are also plotted. In general, the reflectivity spectrum shows strong and broad peaks, e.g., at $\sim$1.91 eV in Fig. 1(a) and $\sim$1.82 eV and $\sim$2.1 eV in Fig. 1(b), which are ascribed to the Fabry-Pérot interference caused by sample structure. Besides, it manifests weak features with peaks and dips at the energies of the excitons associated with conduction and valence confinement subbands around 1.92 eV in Fig. 1(a) and 1.88 eV in Fig. 1(b). In order to accurately determine the energetic positions of the minima of the weak features, a second-order derivative operation[31] is performed on the reflectivity spectrum. The peaks of the second-order derivative of the reflectivity (SODR) correspond to the minima of the weak features in the reflectivity spectrum, as shown in Fig. 1. As the peaks are drastically narrowed, their energies can be accurately determined in the SODR. The overall reproducibility of the energy determination is about ± 0.3 meV for the first two transitions and about ± 1.0 meV for the third one. In general, the reflectivity minima do not necessarily coincide with the exciton resonance accurately, however, the difference in energy is much less than the exciton binding energies.[32,33] We therefore assume in the determination of the exciton transition energies that the maxima in the SODR correspond to excitonic transitions. In this way, the energies of the first three transitions are determined for all the samples.

IV. RESULTS AND DISCUSSIONS

We first check the contribution of the ordering-induced valence-band splitting to the band-gap reduction according to the model. Using the data listed in Table I, we numerically solve Eqs. (3) and (5) for both the disordered ($\eta=0$) and perfectly ordered ($\eta=1.0$) $Ga_xIn_{1-x}P$. With $\Delta^O_{111}(1)=0.20$ eV the contribution is about 20% for $\Delta E_g(1)=-0.32$ eV and decreases to about 16% for $\Delta E_g(1)=-0.405$ eV at $x=0.52$. If the new combination of $\Delta E_g(1)=-0.43$ eV and $\Delta^O_{111}(1)=0.16$ eV is used in the calculation it will further decrease to about 12%. This indicates that the contribution is significantly affected by the $\Delta^O_{111}(1)$ value. Recently, Kippenberg *et al.* deduced a value of about 20% by electroabsorption measurements.[34] Froyen *et al.* calculated a value of about 29% together with $\Delta E_g(1)=-0.35$ eV using the first-principles pseudopotential method within the local-density approximation,[25] but the corresponding $\Delta^O_{111}(1)$ value was not available.

In Fig. 2 the band-to-band transition energies are plotted in lines as functions of the ordering parameter η for lattice-matched ($x\simeq 0.52$, $y=0.52$) and compressively strained ($x=0.4$, $y=0.76$) QW's, respectively, by solving Eq. (7). The values of $\Delta E_g(1)=-0.43$ eV and $\Delta^O_{111}(1)=0.16$ eV are used. Also plotted are the measured transition energies with the following procedure. First, (i) we assume exciton binding energies to be 12 meV,[17] and include them in transferring measured excitonic transition energies to band-to-band values. Then (ii) we fit the first transition energy of each sample to the first theoretical line in Fig. 2 as black squares. This leads to a determination of the ordering parameter η, which is listed in Table III. It is interesting to note here that, even the samples with 6°-$[111]_A$ substrate misorientation are still ordered, though the ordering parameters are significantly smaller than those of samples with other substrate misorientations. Regarding this point, we conclude that attention should be always paid to the ordering in this material system. Finally, (iii) we plot the other two transition energies against this η value into the figure as black dots and triangles, respectively.

There is good agreement for the second transition between the theoretical results and the experimental values. For the third transition, however, the agreement is slightly degraded. An obvious reason is that the third transition in the reflectivity spectrum has a much flatter peak than the first two transitions, which causes a significant uncertainty in resonance energy determination. For the lattice-matched samples the transition energy of the first excited state of the topmost valence subband ($2e$-$2h_1$) is close to that of the ground state of the third valence subband ($1e$-$1h_3$) under a low degree of ordering. The overlap of the two transitions also causes uncertainty in the peak-position determination.

We have also attempted to fit the experimental values with an assumption that the first transition corresponds to a relatively light out-of-plane valence-subband effective mass, i.e.,

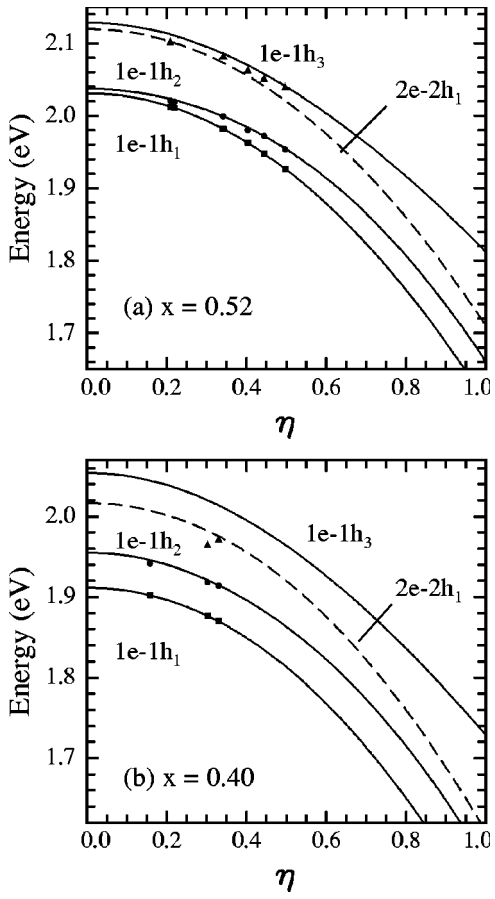

FIG. 2. Band-to-band transition energies as a function of the ordering parameter η for (a) lattice-matched ($x \simeq 0.52$, $y=0.52$) and (b) compressively strained ($x=0.40$, $y=0.76$) $Ga_xIn_{1-x}P/(Al_{0.66}Ga_{0.34})_yIn_{1-y}P$ QW's, respectively. The experimental values are plotted as dots. $1e\text{-}1h_i$ represents the first principal transition between the conduction band and the ith valence subband.

m_{lh}^z listed in Table II, but failed to obtain any agreement. It indicates that the first transition has a relatively heavier out-of-plane effective mass than does the second for all the lattice-matched and compressively strained samples. The upper valence subband is hence hh-like.

For the possible error introduced by the assumed value of the exciton binding energy, we note that the deviation of the assumed value from the real one is only a few meV, which is much smaller than the linewidth (full width at half maximum) of the exciton line in the reflectivity spectrum ($\gtrsim$24 meV). As an estimation, a 3-meV change in the first transition energy results in a $\sim$0.01 change to the η, which falls in the range of ordering scattering in the QW layer.[35] Therefore the determined η can serve as a plausible parameter describing the ordering phenomena in the QW's.

An argument exists maintaining that fitting the energy difference between the first two transitions, ΔE_{12}, to the numerical simulation could also lead to the determination of η. That was indeed the procedure used in the study of $GaInP_2$ bulk material.[36] As the ΔE_{12} is insensitive to the change of η, especially in the compressively strained QW's where a difference of 0.1 in η corresponds to just a $\sim$1.5-meV change in the ΔE_{12} but about a 20-meV change in the $E_{1,1}$, accurate knowledge of the exciton binding energies of the first two transitions becomes crucially important, which is generally difficult to exactly establish in this material system.[37]

In Fig. 3 the energy difference ΔE_{12} from the aforementioned calculation is plotted against the first transition energy $E_{1,1}$ in solid lines for the lattice-matched and compressively strained QW's, respectively. Also depicted is the calculation with $\Delta E_g(1)=-0.47$ eV in dashed lines as well as that with -0.405 eV in dash-dotted lines and that with -0.32 eV in dotted lines, in which the $\Delta_{111}^O(1)$ was selected as 0.20 eV as used by those authors. The experimental data are shown with triangles.

One distinct feature in Fig. 3 is that with the same value of $\Delta_{111}^O(1)$, a larger theoretical value of $-\Delta E_{12}$ corresponds to a smaller ordering-induced band-gap reduction. Another feature is that the experimental values of the $-\Delta E_{12}$ are slightly smaller than the theoretical prediction. A similar phenomenon was also observed in the GaInP bulk alloy and was explained as a result of a clustering-type of short-range order.[12] In our case it is probably caused by the assumption that the first two excitonic transitions have an identical exciton binding energy. According to an ordering-included six-band $\mathbf{k}\cdot\mathbf{p}$ simulation the second transition corresponds to a relatively large in-plane hole effective mass and hence a larger exciton binding energy in compressively strained and lattice-matched QW's. Assuming equality will cause $-\Delta E_{12}$ to be to a degree underestimated. If the difference in the exciton binding energies is accounted for, a slightly downward shifting of the experimental points in Fig. 3 may be expected.

It is clear that for the lattice-matched QW's Wei and Zunger's new values of $\Delta E_g(1)=-0.43$ eV and $\Delta_{111}^O(1)=0.16$ eV lead to a very good description of the experimental data. Ernst *et al.*'s value of $\Delta E_g(1)=-0.47$ eV together with $\Delta_{111}^O(1)=0.20$ eV also provides a good fit. On the other hand, to fit the experimental values to the calculations with $\Delta E_g(1)=-0.405$ eV or -0.32 eV an unreasonably

TABLE III. Ordering parameters for the samples with different substrate misorientation determined by fitting the first band-to-band transition energy $E_{1,1}$ to the theoretical simulations.

	A ($x=0.52$)			B ($x=0.40$)			C ($x=0.52$)		
	0°	6°-$[111]_A$	6°-$[111]_B$	0°	6°-$[111]_A$	6°-$[111]_B$	0°	6°-$[111]_A$	6°-$[111]_B$
$E_{1,1}$ (eV)	1.9623	2.0125	1.9268	1.8761	1.9016	1.8693	1.9818	2.0107	1.9475
η	0.40	0.21	0.50	0.30	0.16	0.33	0.34	0.22	0.44

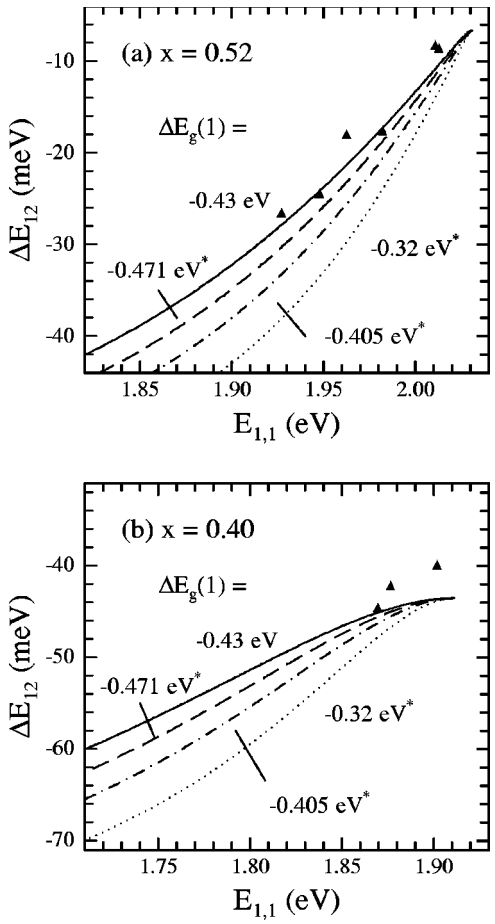

FIG. 3. Correlation between ΔE_{12} and $E_{1,1}$ based on different $\Delta E_g(1)$ values. The experimental data are plotted as triangles. Solid lines are calculated with $\Delta E_g(1) = -0.43$ eV and $\Delta^O_{111}(1) = 0.16$. Dashed lines are of $\Delta E_g(1) = -0.47$ eV, dash-dotted lines of $\Delta E_g(1) = -0.405$ eV, and dotted lines of $\Delta E_g(1) = -0.32$ eV, respectively. The asterisks on the electron-volt values indicate that a $\Delta^O_{111}(\eta = 1)$ value of 0.20 eV was used in the corresponding calculations.

larger difference of ~8 meV or ~11 meV between the two valence subbands' related exciton binding energies has to be assumed. For the compressively strained samples, however, a smaller absolute value of the $\Delta E_g(1)$ is favorable if the aforementioned downward shifting of the experimental points is taken into account. This is in consistent with Geng *et al.*'s observation that relative to lattice-matched QW's, compressively strained QW's manifest less of a band-gap reduction,[38] and may suggest that effects of (111) atomic ordering in compressively strained QW's is weakened due to the interaction with the (001) elastic strain.

To check the influence of using different values of the deformation potentials, we repeat the procedures involved in plotting Fig. 2 and Fig. 3 with the a_v and a_c listed in the parentheses of Table III. We note that the calculated transition energies for the lattice-matched QW's are nearly the same as those plotted in Fig. 2(a). The determined ordering parameters just change by an amount of ~0.005, which is in the range of the ordering scattering in the QW layer.[35] On the other hand, the calculated transition energies for the compressively strained QW's are slightly reduced (~8 meV), which lead to a reduction in the ordering parameters of ~0.03 for the samples with 0° and 6°-$[111]_B$ substrates and of ~0.07 for the sample with the 6°-$[111]_A$ substrate. The reduction of the transition energies due to using the new deformation potentials may become critical for the compressively strained QW's with very low ordering. In a measurement of an additional sample with $x = 0.40$ and 6°-$[111]_A$ substrate, we observe an excitonic transition energy of 1.9032 eV for the first transition. To fit the calculation using the new values of the deformation potentials, we have to either assume the exciton binding energy to be as low as 1 meV or reduce the *z*-direction electron effective mass to $< 0.05 m_0$ to warrant $\eta \geqslant 0$, neither of which is reasonable. Nevertheless, using the new values of the a_v and a_c does not change the above conclusions on the favorable values of the $\Delta E_g(\eta)$ and $\Delta^O_{111}(\eta)$ for the lattice-matched and compressively strained QW's. As an example a similar plot of Fig. 3(b) is depicted in Fig. 4. Obviously, here again a small absolute value of the $\Delta E_g(1)$ (e.g., -0.32 eV) is preferred if the aforementioned downward shifting of the experimental points is taken into account. On this point, the widely used values of the deformation potentials seem to be favorable and will be used in the following discussion.

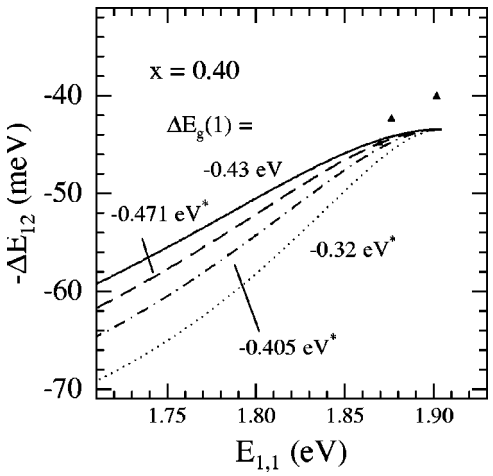

FIG. 4. Similar to Fig. 3, except that here the new values of the a_v and a_c deformation potentials listed in the parentheses of Table III are used in the calculations.

Being sure that the model can reasonably predict the band-to-band transitions in the ordered $Ga_xIn_{1-x}P/(Al_{0.66}Ga_{0.34})_yIn_{1-y}P$ QW's, we now set our sights on the band offset. We solve Eqs. (6) numerically, and plot the band-offset ratio as a function of strain and ordering parameter, respectively, in Fig. 5. It is clear that ordering causes the conduction-band-offset ratio to increase, and the upper valence-subband-offset ratio to decrease. For perfect ordering, $Q_c \sim 0.71$ for $x = 0.40$ and $Q_c \sim 0.72$ for $x = 0.52$. Meanwhile, ordering removes the cusp in Fig. 5(b) at $x \sim 0.52(\epsilon = 0)$ for $\eta = 0$, which is caused by E_{lh} and E_{hh} switching order.[12]

The results for the disordering suggest a nearly constant conduction-band-offset ratio $Q_c \simeq 0.58$ for lattice matched and compressively strained, but a significant drop for tensile

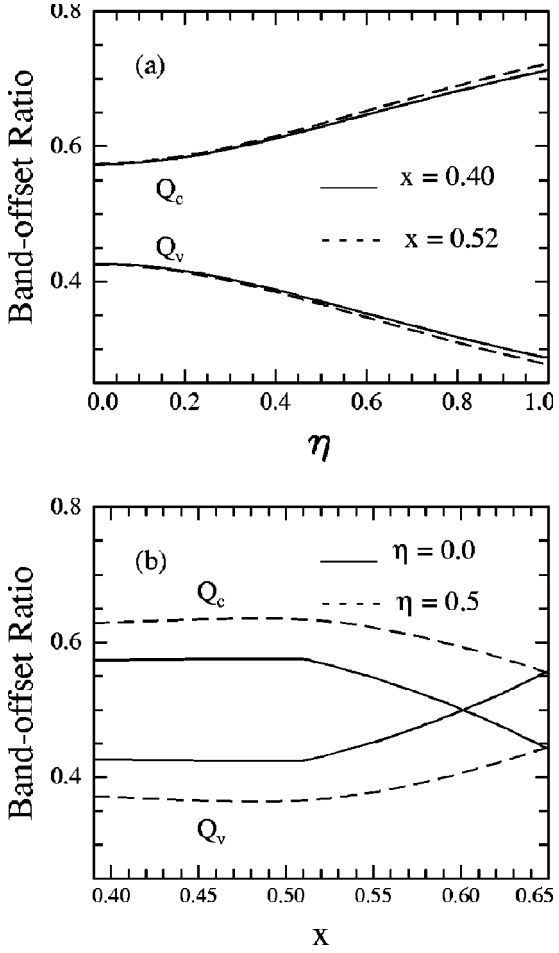

FIG. 5. Band-offset ratios as a function of (a) ordering parameter, and (b) strain for $Ga_xIn_{1-x}P/(Al_{0.66}Ga_{0.34})_{0.52}In_{0.48}P$ QW's.

strained QW's. It is in good agreement with the results given in Ref. 28 predicted by the Krijn formalism of the model-solid theory.[23] A small difference, if that exists, is due to the fact that different material parameters were used. Our Q_c is also consistent with Liedenbaum *et al.*'s experimental value $Q_c=0.60\pm0.05$ for $Ga_xIn_{1-x}P/(Al_{0.66}Ga_{0.34})_{0.52}In_{0.48}P$ QW's obtained by fitting of PLE spectra with the $\mathbf{k}\cdot\mathbf{p}$ calculation,[16] and slightly smaller than Kowalski *et al.*'s value of $Q_c=0.65$ for $GaInP/(Al_{0.66}Ga_{0.34})_{0.52}In_{0.48}P$ determined by pressure-dependent photoluminescence measurements.[20]

However, the Q_c value is obviously smaller than Dawson *et al.*'s prediction of 0.67 for $x=0.44$ and 0.70 for $x=0.59$ $Ga_xIn_{1-x}P/AlGaInP$ QW's,[18,28] though identical material parameters are used. An obvious reason for tensile strained QW's is that the definition of Q_c is different from that used in Ref. 28. We have employed a similar definition to that proposed by Krijn, while Dawson *et al.* defined $Q_c=\Delta E_c/(\Delta E_c+\Delta E_{hh})$, where ΔE_{hh} is the confinement energy of the heavy-hole subband, which leads Q_c to a larger value in the range of tensile strain. In fact a value of $Q_c\simeq0.57$ can be derived for $Ga_{0.59}In_{0.41}P/AlGaInP$ QW's if Dawson *et al.*'s definition is used in our calculation. Another important reason is that those Q_c values were determined to be an adjustable parameter in fitting of the ΔE_{12} observed in QW's by assuming identical binding energy to the hh and lh excitons. As aforementioned, the general trend of lh-exciton binding energy is that it is larger than that of the corresponding hh-exciton made $-\Delta E_{12}$ underestimated in compressively strained QW's (equivalent to the hh-lh splitting defined in Ref. 18). Due to the fact that the hh band has a heavier out-of-plane effective mass, this will result in an underestimation of Q_v and hence an overestimated Q_c. On the other hand for tensile strained QW's it caused an overestimation to $-\Delta E_{12}$ (equivalent to the lh-hh splitting in Fig. 4 of Ref. 28) and hence an overestimated Q_c, again due to the difference in the out-of-plane effective masses of hh and lh bands. This indicates that to use the ΔE_{12} in evaluating parameters in QW's, the exciton binding energies should be accurately known in advance.

V. SUMMARY

To summarize, we have incorporated the ordering effects of band-gap reduction and valence-band splitting into model-solid theory to account for both strain and ordering effects on QW electronic band structures. We have also measured ordered and strained/lattice-matched $Ga_xIn_{1-x}P/(Al_{0.66}Ga_{0.34})_yIn_{1-y}P$ QW samples by low-temperature optical reflectivity spectroscopy to determine excitonic resonance energies. The results indicate that the model can reasonably predict band-to-band transitions in ordered $Ga_xIn_{1-x}P/(Al_{0.66}Ga_{0.34})_yIn_{1-y}P$ QW's. The ordering parameter in QW's can be estimated with the first band-to-band transition energy. The $E_g(1)$ is strain dependent, whereas $\Delta E_g(1)=-0.43$ eV gives a best fit for the lattice-matched QW's; a smaller absolute value of $\Delta E_g(1)$ is favorable for the compressively strained samples. Compressive strain tends to weaken the ordering effects. Ordering causes the conduction-band-offset ratio to increase. For lattice-matched and compressively strained QW's, Q_c falls into a range of $0.58-0.72$ as η changes from 0 through 1. For disordered and lattice-matched/compressively strained $Ga_xIn_{1-x}P/(Al_{0.66}Ga_{0.34})_{0.52}In_{0.48}P$ QW's, Q_c has a nearly constant value of $Q_c\sim0.58$.

ACKNOWLEDGMENTS

One of the authors (J.S.) thanks the Volkswagen-Stiftung and the Deutscher Akademischer Austauschdienst for financial support.

*Author to whom correspondence should be addressed. Electronic address: jshao@mail.sitp.ac.cn

[1] E.P. O'Reilly, G. Jones, A. Ghiti, and A.R. Adams, Electron. Lett. **27**, 1417 (1991).
[2] A. Moritz, R. Wirth, S. Heppel, C. Geng, J. Kuhn, H. Schweizer, F. Scholz, and A. Hangleiter, Appl. Phys. Lett. **71**, 650 (1997).
[3] R.W. Herrick and P.M. Petroff, Appl. Phys. Lett. **72**, 1799 (1998).
[4] P.M. Smowton, P. Blood, and W.W. Chow, Appl. Phys. Lett. **76**,

1522 (2000).
[5] S.-H. Wei and A. Zunger, Phys. Rev. B **39**, 3279 (1989).
[6] S.-H. Wei and A. Zunger, Appl. Phys. Lett. **56**, 662 (1990).
[7] D.B. Laks, S.-H. Wei, and A. Zunger, Phys. Rev. Lett. **69**, 3766 (1992).
[8] S.-H. Wei, D.B. Laks, and A. Zunger, Appl. Phys. Lett. **62**, 1937 (1993).
[9] G.S. Horner, A. Mascarenhas, S. Froyen, R.G. Alonso, K. Bertness, and J.M. Olson, Phys. Rev. B **47**, 4041 (1993).
[10] R.B. Capaz and B. Koiller, Phys. Rev. B **47**, 4044 (1993).
[11] S.-H. Wei and A. Zunger, Appl. Phys. Lett. **64**, 757 (1994).
[12] S.-H. Wei and A. Zunger, Phys. Rev. B **49**, 14 337 (1994).
[13] P. Ernst, C. Geng, F. Scholz, H. Schweizer, Y. Zhang, and A. Mascarenhas, Appl. Phys. Lett. **67**, 2347 (1995).
[14] P. Ernst, C. Geng, G. Hahn, F. Scholz, H. Schweizer, F. Phillipp, and A. Mascarenhas, J. Appl. Phys. **79**, 2633 (1996).
[15] O.P. Kowalski, J.W. Cockburn, D.J. Mowbray, M.S. Skolnick, M.D. Dawson, G. Duggan, and A.H. Kean, Phys. Rev. B **53**, 10 830 (1996).
[16] C.T.H.F. Liedenbaum, A. Valster, A.L.G.J. Severens, and G.W. 't Hooft, Appl. Phys. Lett. **57**, 2698 (1990).
[17] J.R.P. Schneider, R.P. Bryan, E.D. Jones, and J.A. Lott, Appl. Phys. Lett. **63**, 1240 (1993).
[18] M.D. Dawson and G. Duggan, Appl. Phys. Lett. **64**, 892 (1994).
[19] M.D. Dawson and G. Duggan, Phys. Rev. B **47**, 12 598 (1993).
[20] O.P. Kowalski, J.W. Cockburn, D.J. Mowbray, M.S. Skolnick, R. Teissier, and M. Hopkinson, Appl. Phys. Lett. **66**, 619 (1995).
[21] F. Scholz, C. Geng, M. Burkard, H.-P. Gauggel, H. Schweizer, R. Wirth, A. Moritz, and A. Hangleiter, Physica E (Amsterdam) **2**, 8 (1998).
[22] C.G. Van de Walle, Phys. Rev. B **39**, 1871 (1989).
[23] M.P.C.M. Krijn, Semicond. Sci. Technol. **6**, 27 (1991).
[24] T.Y. Wang and G.B. Stringfellow, J. Appl. Phys. **67**, 344 (1990).
[25] S. Froyen, A. Zunger, and A. Mascarenhas, Appl. Phys. Lett. **68**, 2852 (1996).
[26] S.-H. Wei and A. Zunger, Phys. Rev. B **57**, 8983 (1998).
[27] C. Geng, Ph.D. thesis, University of Stuttgart, 1997.
[28] M.D. Dawson, G. Duggan, and D.J. Arent, Phys. Rev. B **51**, 17 660 (1995).
[29] S.-H. Wei and A. Zunger, Phys. Rev. B **60**, 5404 (1999).
[30] P. Emanuelsson, M. Drechsler, D.M. Hofmann, B.K. Meyer, M. Moser, and F. Scholz, Appl. Phys. Lett. **64**, 2849 (1994).
[31] J. Shao, D. Haase, A. Dörnen, V. Härle, and F. Scholz, J. Appl. Phys. **87**, 4303 (2000).
[32] B.V. Shanabrook, O.J. Glembocki, and W.T. Beard, Phys. Rev. B **35**, 2540 (1987).
[33] A.F. Terzis, X.C. Liu, A. Petrou, B.D. McCombe, M. Dutta, H. Shen, D.D. Smith, M.W. Cole, M. Taysing-Lara, and P.G. Newman, J. Appl. Phys. **67**, 2501 (1990).
[34] T. Kippenberg, J. Krauss, J. Spieler, P. Kiesel, G.H. Döhler, R. Stubner, R. Winkler, O. Pankratov, and M. Moser, Phys. Rev. B **60**, 4446 (1999).
[35] J. Shao, A. Dörnen, R. Winterhoff, E. Baars, and F. Scholz (unpublished).
[36] P. Ernst, Y. Zhang, F.A.J.M. Driessen, A. Mascarenhas, E.D. Jones, C. Geng, F. Scholz, and H. Schweizer, J. Appl. Phys. **81**, 2814 (1997).
[37] D. Kinder, S.L. Wong, A.N. Priest, R.J. Nicholas, G. Duggan, M.D. Dawson, S.P. Najda, and A.H. Kean, Solid-State Electronics **40**, 597 (1996).
[38] C. Geng, M. Moser, R. Winterhoff, E. Lux, J. Hommel, B. Höhing, H. Schweizer, and F. Scholz, J. Cryst. Growth **145**, 740 (1994).